

Local process investigations on composite electrodes: on the way to understanding design criteria for spray coated anodes in Zn electrowinning

by S. Schmachtel*†, S.E. Pust‡, M. Toiminen*, G. Wittstock‡, K. Kontturi*, O. Forsén†, and M.H. Barker§

Synopsis

Several possible physico-chemical properties of composite electrodes for oxygen evolution are presented to describe experimental data for which a mathematical model had been developed. On this basis, local electrical and electrochemical properties of a composite electrode were investigated with conductive atomic force microscopy (CAFM) and scanning electrochemical microscopy (SECM). It could be shown by CAFM measurement that the boundary between matrix and catalyst particles seemed to have special advantageous electrical properties.

The SECM measurements showed the presence of mass transport phenomena with increased surface concentrations, whilst the thickness of the Nernst diffusion layer was very small. An intermediate was detected and assigned to be hydrogen peroxide. From all species involved in the oxygen evolution reaction (H_2O_2, H^+ and O_2), it was concluded that local active spots exist on the electrode on which hydrogen peroxide reacts to oxygen and protons. A two–step two-material process was suggested to explain the whole oxygen evolution mechanism.

Introduction/background

Oxygen evolution is the common counter-reaction for electrowinning of metals from sulphide ores.

While Zn is almost exclusively produced via this method, only about 10% of the copper produced is gained via solvent extraction and electrowinning methods.

Also Co, Ni and Cd are partially electrowon as main or side products[1] employing oxygen evolution as counterreaction:

$$H_2O \rightarrow 1/2O_2 + 2H^+ + 2e^- \quad [1]$$
$$E = 1.23V \text{ vs. } SHE$$

This reaction is connected to high overpotentials, which are in Zn electrowinning about 800 mV, or 20–25% of the total cell voltage, and with that an equal amount of the total electrical energy[1]. Many attempts have been made to reduce the overpotential by introducing better catalysts. The main anode systems are nowadays all lead based[1], which offer the best cost:value ratio for most of the industrial processes that employ oxygen evolution.

The most famous approach for improvements, the dimensionally stable anode (DSA™[2,3]), which is a titanium metal electrode covered with mixed metal oxides (MMO, which are mostly precious metals) is usually applied only in a few cases where metals are electrowon from chloride solutions. They can be also used in Cu electrowinning after the solution has been cleaned by solvent extraction.

In zinc electrowinning, however, the DSA suitable for oxygen evolution has shown to fail after a few days because the manganese content of the solution leads to MnO_2 growth in between the electrode base material and the active coating, which is then flaked off[4].

Most of the scientific approaches in that area are using the same precious mixed metal approach, where metal salts are repeatedly applied to the surface of a titanium electrode and decomposed to metal oxides. The process is very complex, it influences the performance of the anode substantially and, also because of the time consuming process in both research and manufacturing, it is very expensive[5].

Due to the high risk (high investment costs) and due to the impurities present, DSA anodes have not really found their way into modern tank houses, although they have been very successful in the chlor-alkali industry[5].

*† *Laboratory of Physical Chemistry and Electrochemistry, Helsinki University of Technology, Finland.*

† *Laboratory of Materials Chemistry and Corrosion, Helsinki University of Technology, Finland.*

‡ *Centre of Interface Science, Department of Pure and Applied Chemistry and Institute of Chemistry and Biology of the Marine Environment, Carl von Ossietzky University Oldenburg, Germany.*

§ *Outotec Research Centre, Pori, Finland.*

© *The Southern African Institute of Mining and Metallurgy, 2008. SA ISSN 0038–223X/3.00 + 0.00. This paper was first published at the SAIMM Symposium,* Lead & Zinc 2008, *25–29 February 2008.*

The available lead based technologies are cheap and well known and, although replacing lead by other electrode systems would probably save a lot of energy, the main improvements have been made only on the basis of lead alloying with Ca, Sn, Ag, Co and others[6,7].

There have been two attempts to establish a commercial anode product that is based on a composite electrode system: the Merrlin anode[8,9] and a porous titanium electrode filled with lead[10]. Both systems have been described as being successful in reducing the anode potential and suffering less corrosion. Nevertheless they have not yet been widely applied.

A new method is under development at Outotec Oyj, Finland, which aims to find an alternative approach for MMO coated electrodes, but with cheaper materials and a cheaper manufacturing method, which employs spraying of catalytic coatings onto a standard lead based anode.

A spray coating method is much faster and more easily applied compared to the procedures for manufacturing a DSA or a Merrlin anode[8,9] (anode coated with a high pressure method) or the sintered porous titanium electrode[10].

In our tests, cold spraying[11] has shown to be superior to high velocity oxygen flame (HVOF) spraying, because as a low temperature process it does not alter the properties of the catalyst and it does not warp the electrode. From our laboratory-scale tests it could be concluded that cold spray coated electrodes were more active than the HVOF coated counterparts. Additionally, cold spraying equipment is in principle relatively cheap and very easy to handle.

Properties of composite electrodes

Composite electrodes could be a possible solution for facing the harsh conditions found especially in Zn electrowinning. The two components of the electrode (matrix and catalyst) can be combined[12] in such a way to overcome the main problems of anode materials.

Corrosion and the high overvoltage can be lowered by introducing catalyst particles into the metal matrix, thereby reducing the required anodic potential and with that the corrosion of the matrix material.

The matrix, on the other hand, could be used to ensure the electrical contact to the catalyst particles, especially when the catalyst is not a very good conductor (the matrix metals are usually much better conductors than the metal oxide catalysts [13]).

The sprayed coating on lead anodes resembles composite electrodes in that the catalyst particles are accelerated by air, shot into the lead surface and buried into it. By testing the catalyst in composite electrodes it is possible to simulate certain properties of the coating: the influence of catalyst fraction and size of the catalyst particles can be investigated by pressing known mixtures of matrix materials and catalyst powder into a composite electrode tablet[14].

Additionally, the testing method also offers an effective screening method for catalysts without having to produce a full-size, which makes catalyst development easier. This overall *ex situ* preparation approach of the catalyst is, to our knowledge, a new method for catalyst development and simplifies the engineering process of such systems.

Although composite electrodes have been proposed for gas evolution reactions and have been studied extensively by Musiani *et al.*[12], to our knowledge, it is not exactly known how the key properties of a composite electrode (size and fraction of the catalyst, statistics of the catalyst distribution) affect the performance of such electrode systems, and what physicochemical processes (mass transport, gas evolution, three phase boundary properties, conductivity issues) are influenced in which way.

Results from earlier electrochemical tests

In earlier electrochemical tests, we investigated the catalytic ability of different MnO_2 modifications in composite electrodes, which were made up with Pb in powder form. The resulting mixture was compacted in a press to obtain electrode tablets, which were inserted into a special holder for testing. A detailed description of the set-up and the experimental conditions are found in[14].

All of the composite electrodes were more active than plain lead electrodes (1350 mV vs. SSE at 600Am^{-2}[7]); however, the different modifications behaved differently, where CMD (chemically prepared manganese dioxide) was most active, and β-MnO_2 was least active (Figure 1).

This emphasizes the catalytic ability of MnO_2 to enhance the oxygen evolution reaction; however, the right modification has to be chosen. Thermally prepared coatings lead to β-MnO_2, while the catalyst formed on top of lead electrodes during Zn and Cu electrowinning is γ-MnO_2 in the form of a thickly grown bulky layer loosely adhering to the lead electrode substrate.

Although reducing the corrosion of the lead electrode and its voltage in general, the layer has several disadvantages: it flakes off, erodes the lead surface by removing part of it, can produce short circuits to the cathode, and thus has to be cleaned regularly.

While all of the composite electrodes showed lower electrode potentials than the layer present in Zn electrowinning[7], the saving with the application of CMD could be at best in the order of 250 mV or 5–10% of the total electrical energy input.

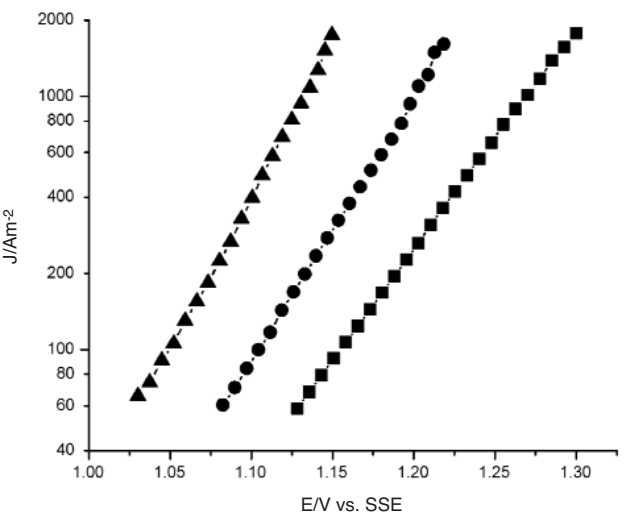

Figure 1—Tafel plot for different MnO_2 materials in composite electrodes at 5 wt%. ▲ CMD ● EMD (electrochemically prepared MnO_2) ■ β-MnO_2

The reason that both systems are so different could be due to the difference between the composite electrode and the MnO_2 layer in Zn electrowinning. This was the reason why we investigated the effects of volume percentage and size of the catalyst in more detail.

The catalyst (CMD) was mixed in different mass fractions to the lead powder to analyse the effect of increased catalyst volume content. For size analysis the catalyst was sieved into 4 different size fractions, which were mixed into lead at 10 weight per cent of catalyst.

The results show that increasing the volume content of catalyst has its limitations, the increase from 15% on is nonlinear and is affected by difficulties of reproducibility. (Figure 2)

The size relationship, however, more closely resembles an inverse proportional relationship (Figure 3).

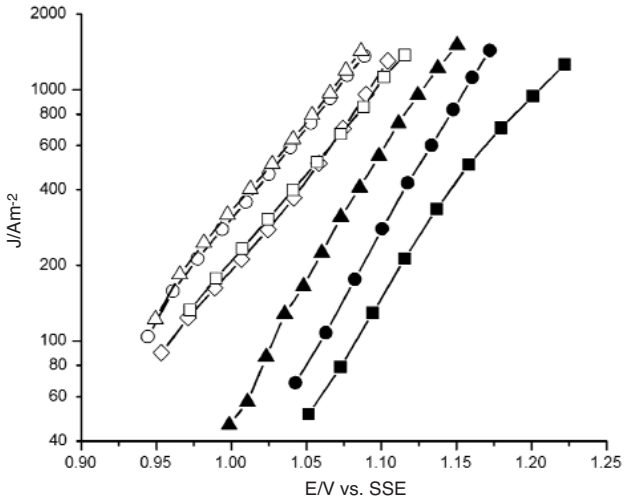

Figure 2—Effect of the wt% on the performance of the composite electrode for CMD (■ 3% ● 5% ▲ 10% ◇ 15% □ 20% ○ 25% △ 30%)

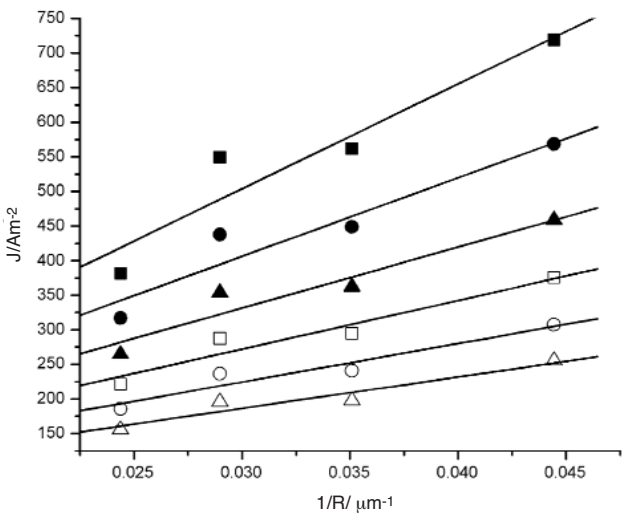

Figure 3—The effect of the mean CMD particle size (22.5, 28.5, 34 and 41 µm) on the current density (CMD electrode). The symbols refer to different iR corrected potentials (■ 1.10V ● 1.09V ▲ 1.08V □ 1.07V ○ 1.06V △ 1.05V)

Initially, the relationships seem logical. However, on closer examination, it is unreasonable why there is a limit to the increase in the surface percentage (although the tablets are still mechanically stable as such). The 1/r relationship is especially difficult to understand. Replacing fewer bigger particles with more smaller ones, although their geometrical area fraction remained the same, had substantial effect on the performance for such small variations.

The fact that the effect is dependent on the current density does not allow us to conclude that it depends on different surface chemical properties (like active surface area fraction or surface chemistry). It further suggests that the changes are due to variations in the distribution of the active areas in the composite electrode.

We believe that the presented relationships might have something to do with possible special physicochemical properties of composite electrodes, which are presented in the next section.

Possible physicochemical processes on composite electrodes under oxygen evolution

The overall physicochemical system in combination with composite electrodes is very complex, as there could be many processes involved at the same time. Several possible processes are presented and analysed whether they could affect the performance of composite electrodes in general, and whether their effects have an impact on the particular case presented.

There are several aspects that should be considered to be important for a composite electrode (Figure 4):

The composite or the coating has to be mechanically stable. Assuming spherical catalyst particles, the maximum volume load of catalyst is that of a closed packed arrangement (74.05%[15]). In practice, however, there has to be enough matrix material gluing the catalyst together, which is probably well below that highest possible fraction, since the gas evolution requires good mechanical properties.

Electrical properties are, as well as the mechanical properties, dependent on sufficient metal matrix content. Additionally, the surface catalyst particles have to be well connected to the electrical network of the matrix metal. Since most of the electrons will pass through the boundary (MnO_2 is not a good conductor), the boundary is most active. This is due to other electrons suffering an additional potential drop passing through the resistive catalyst particle.

Since protons and oxygen are generated in the reaction, they have to be transported away from the electrode into the bulk solution. This is usually helped by the convection that is induced by the gas bubbles passing by the electrode. The stagnant layer at the electrode is thus small.

Proton diffusion away from the electrode is slowed down since a supporting electrolyte is not present and electroneutrality has to be fulfilled. This leads protons diffusing together with hydrogen sulphate ions, or as sulphuric acid, which has a much slower diffusion constant.

Oxygen dissolves first as molecular oxygen, and at high supersaturation[16] bubbles are formed, which transport the oxygen away.

Microelectrodes show high mass transport rates due to strong edge effects, where the current passes mainly through the edges. As a random arrangement of microelectrodes,

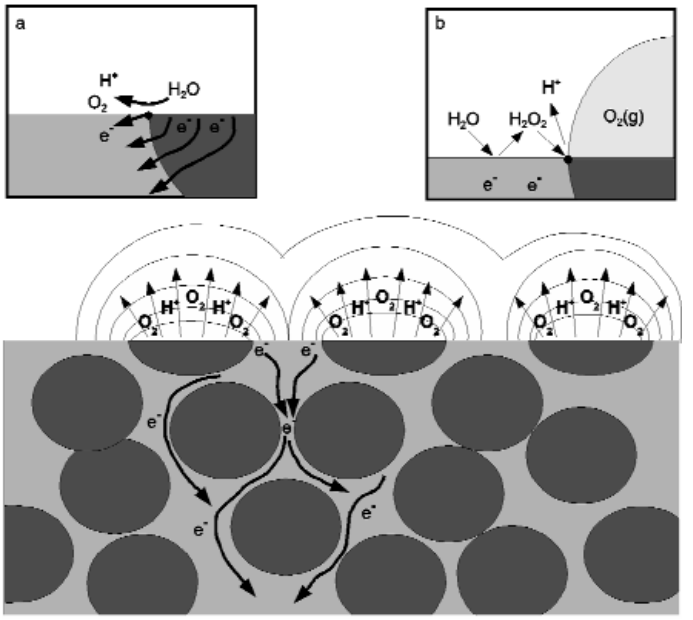

Figure 4—Processes at the composite electrode in cross-section. Electrons have to pass through the matrix material to the back contact of the electrode. At the surface (a) the electrons have to pass through the catalyst particle into the matrix causing an additional potential drop. The protons and oxygen have to be transported away from the electrode and build up an overlapping diffusion profile. (b) shows two special cases: water reacts to H_2O_2 on Pb and reacts further on the catalyst to oxygen gas. A bubble is growing on the catalyst particle and screens everything except the boundary

however, they display a special behaviour of mass transport, in which the diffusion fields of all microelectrodes/catalyst particles form a complex overlap (if the spots are not too far apart). From the electrode towards to the bulk solution the diffusion field smoothes, and after some distance forms a linear diffusion profile[17].

Albeit the overlapping, the edge effects still lead to the highest currents at the edges of all catalyst spots. The performance of the anode/electrode thus also depends on the size and fraction of the catalyst particles, their distances from each other, and on the size of the stationary Nernst diffusion layer.

The boundaries between catalyst and matrix material can be seen as three phase boundaries (matrix, catalyst and electrolyte). Such types of boundaries are usually highly reactive spots. They can function as nucleation spots for gas bubbles, and they can also be the place of special two-step two-material reactions: an intermediate is formed at one component of the electrode and reacts further on the other part of the electrode.

Gas evolution is another aspect which is influenced by the alternating properties of the composite electrode: due to different surface energies, the bubbles will prefer to sit on the more hydrophobic sites and it will be difficult to move them over matrix catalyst boundaries. A bubble sitting on a catalyst particle will thus spread to cover the whole area of the particle and maybe even depart before it expands onto the matrix material.

These possible conditions emphasize the special situation at the matrix catalyst boundaries. All of the presented situations could be combined to give a complex overall system, which has tuneable physicochemical properties (catalyst fraction and size, matrix and catalyst material). There are thus good reasons to believe that a combination of all effects leads to the increase in performance, which is visible in the experimental results presented.

The overall process can be well described with a mathematical model based on the premise that the current passes exclusively through the boundary[14]:

$$i = nFAk(E)\frac{vol\%}{r_p} \qquad [2]$$

where i is the total current, A the electrodes geometric surface area, n the number of electrons involved, F the Faraday constant, $k(E)$ a potential dependent electrochemical rate constant, r_p the catalyst particle radius and vol% the catalyst volume fraction.

Studies of the local processes with the help of conductive atomic force microscopy (CAFM) and scanning electrochemical microscopy (SECM)

Introduction to the techniques

Conductive atomic force microscopy (CAFM)[18] is an extension of the conventional atomic force microscopy (AFM); the cantilever and the tip are conductive and can be connected to one outer voltage, while the sample is connected to 0V. By applying a potential, the current passing through the surface can be measured and laterally resolved.

Scanning electrochemical microscopy (SECM)[19] belongs to the scanning probe microscope family, where usually an ultra microelectrode (UME) is scanned across the electrolyte above the sample.

Usually the experiment is carried out such that the measured Faraday current signal (reaction of a specific electrochemically active species) is also dependent on the surface reaction rates. With that the local surface reactivity of surfaces can be determined.

Local process investigations on composite electrodes

There are mainly two different working modes in SECM. In the feedback mode, the substrate/sample is not polarized and the tip current is dependent on the location of the tip. When the tip approaches the sample, the diffusion field of the ultra micro electrode (UME) is altered, the measured current changes.

This happens either by the substrate obstructing the mass transport (inactive sample or 'negative feedback'), or increasing the reactants concentration by a back-reaction at the substrate, from which a 'positive feedback' follows (active sample).

The second mode is a generation collection mode, where the sample is also polarized. The generation of reactive species happens either at the microelectrode and is detected at the sample (tip generation substrate collection mode) or, more commonly, the sample generates species, which are detected at the microelectrode tip (substrate generation tip collection mode) (Figure 5).

In our work we have exclusively used the substrate generation tip collection mode to measure the diffusion fields of the composite electrodes under polarization. Here, we utilize the fact that the tip current is proportional to the species' concentration around the tip. The current signal can thus be directly translated to concentration with a suitable calibration and without difficult calculations.

In this mode, however, a feedback interaction is unwanted, because it can either accelerate or decelerate the local surface reaction, or the diffusion field of the microelectrode can be impeded. Signals from close distances to the sample thus have to be regarded with caution.

CAFM results

Both the contact mode image and CAFM image of one catalyst spot were recorded with a Digital Instruments Dimension 3100 with a NanoScope IIIa Controller, a Quadrex extension box, and a CSFM application module (Veeco, USA). Before imaging the pressed tablet sample (10 weight% CMD14) was polished with a Al_2O_3 suspension.

A diamond-like carbon tip was used due to its excellent wear resistance so that an exact contact mode image could be recorded simultaneously with the CAFM image. The AFM image and the CAFM image ($\triangle E$ = +500 mV (sample against tip) = anodic polarization) can both be seen in Figure 6.

The contact mode image shows that the particle is not completely flush with the surface of the composite electrode and has a relatively high aspect ratio. The CAFM picture can give only semi-quantitative information, because of the usage of the DLC tip with very complex semiconducting properties. Nevertheless, it can be seen that the current though the tip was highest at the particle matrix boundary.

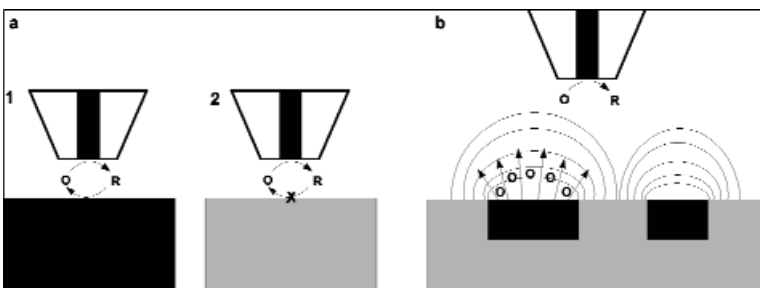

Figure 5—The two main SECM modes: (a) feedback mode: (1) The concentration of O/tip current increases on approach by R reacting back to O on the substrate (black electrode, positive feedback) (2) On approach the diffusion of O to the micro electrode is blocked by the surface (substrate is inactive, negative feedback) (b)substrate generation tip collection mode: the tip is used as a local concentration sensor, ideally not influencing the substrate and its diffusion field

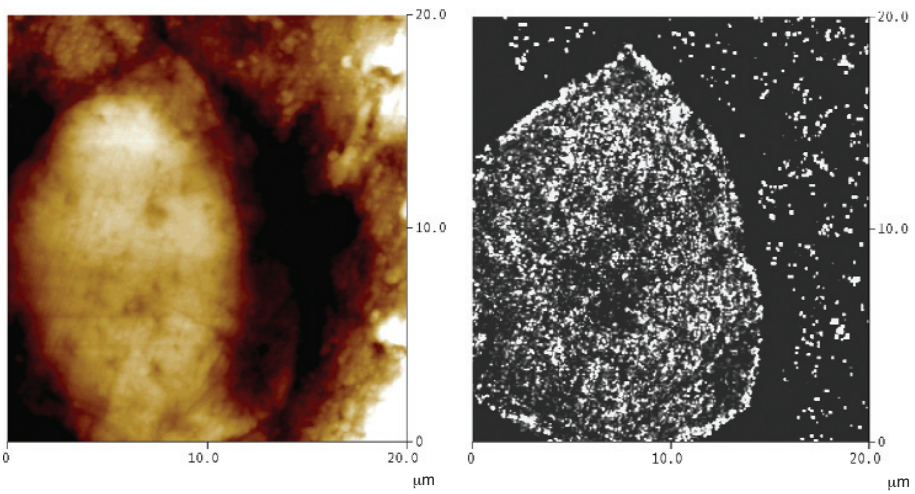

Figure 6—Contact mode image (left, hmax=600 nm) and CAFM image (right, $\triangle E$ = +500 mV)

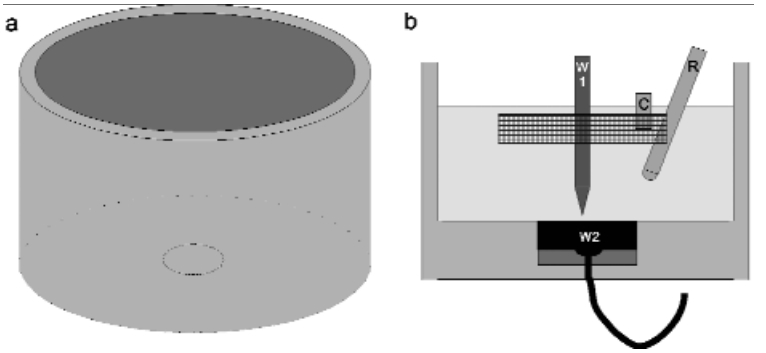

Figure 7—Set-up and cell for SECM measurements: (a) cell as a PVC beaker with a hole at the bottom (b) cross-section of the filled cell: platinum mesh as counter electrode (C), Ag/AgCl reference electrode (R), ultramicroelectrode (W1) and composite electrode (W2)

SECM experiments and results

The pressed tablet sample (10 weight% CMD[14] using the sieved fraction with r>45 μm) was inserted into a home-made PVC cell (ca. 100 ml volume, Figure 7) which had a hole to insert the tablet with its wire at the bottom. The tablet was glued into the hole with nail lacquer, which could be removed later with acetone. The testing solution was 2M H_2SO_4 at room temperature (ca. 20°C).

For the testing a platinum mesh and an Ag/AgCl reference electrode were used. The UME was a home-made 5 μm Pt tip with a small RG value. The potentials were controlled with the help of a CHI7001B bipotentiostat (CH Instruments, USA), while the system controlling the position of the UME was home-built and is described by Wittstock *et al.*[20]. All images were generated with the help of the MIRA imaging software[21].

After 1 hour of preconditioning the tablet at 1.8 V vs. Ag/AgCl, a potential was applied to the UME (-0.3 V vs. Ag/AgCl), waiting 10 min. for the UME to reach steady state. The surface of the sample was approached carefully under hydrogen evolution at the tip (Figure 8).

After that, the tip was retracted by 25 μm and the tilt was removed by slow subsequent surface line scans: whenever the surface seemed to lower onto the surface the tip was further retracted before the sample table was adjusted with precision gauges. After that the tip was approached and retraced again to 25 μm distance until it was certain that the tip was about 25 μm above the surface and the line scan was in the horizontal plane of the sample. At the end of the alignment procedure the tip was retracted by 250 μm.

For acquisition of an image, the sample potential was lowered to 1.675 V vs. Ag/AgCl and a YZ scan from 275 μm to 25 μm above the sample was recorded for 3 different tip potentials referring to the detection of protons (-0.3 V), oxygen (-0.05 V) and H_2O_2 (1.1 V vs. Ag/AgCl):

After 10 min. equilibration of both microelectrode and sample to the applied potentials, the diffusion layer was scanned at constant height above the surface (forward and backward) followed by stepping the microelectrode 5 μm downwards until the level of 25 μm was reached.

The following reactions should happen at the UME at the respective potentials:

$$O_2 + 2H^+ + 2e^- \rightarrow H_2O \quad E = 1.23V \text{ vs. } SHE \; E_{UME} = -0.05V \text{ vs. } Ag/AgCl \qquad [3a]$$

$$2H^+ + 2e^- \rightarrow H_2 \quad E = 0V \text{ vs. } SHE \; E_{UME} = -0.3V \text{ vs. } Ag/AgCl \qquad [3b]$$

$$H_2O_2 \rightarrow O_2 + 2H^+ + 2e^- \; E = 0.70V \text{ vs. } SHE \; E_{UME} = 1.1V \text{ vs. } Ag/AgCl \qquad [3c]$$

Hydrogen peroxide production might happen on the composite electrode with the following reaction:

$$2H_2O \rightarrow O_2 + H_2O_2 + 2H^+ + 2e^- \qquad [4]$$

At -0.3 V both oxygen content and proton concentration should contribute to the measured current; however, the oxygen content is very small compared to the proton concentration (solubility of about 0.5 mmol/ℓ for water[22], and a similar value for H_2SO_4[23]). Thus it can be approximated to have only a negligible influence on the measurement of proton concentration. The oxygen reduction at -0.05 V does not occur simultaneously with hydrogen evolution.

Diffusion profiles

The diffusion profiles recorded can be seen in Figure 9. Both proton and oxygen concentrations increase towards the electrode, as expected. What is particularly interesting is that

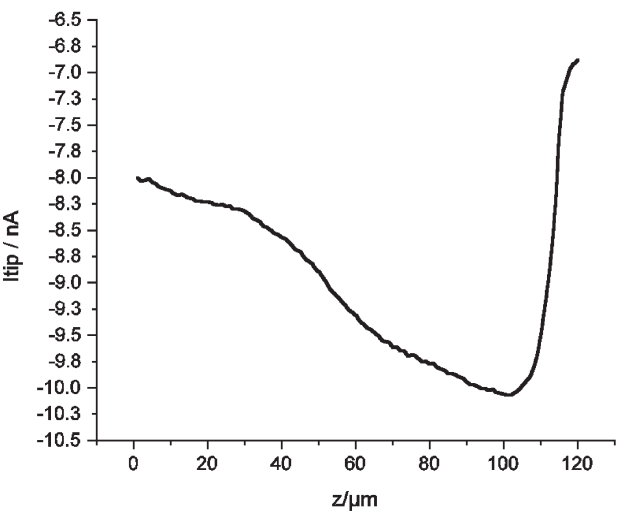

Figure 8—UME approach to the surface. The proton reduction current increases first and near the sample the diffusion of protons towards the sample is obstructed by the substrate; at the end the surface is touched

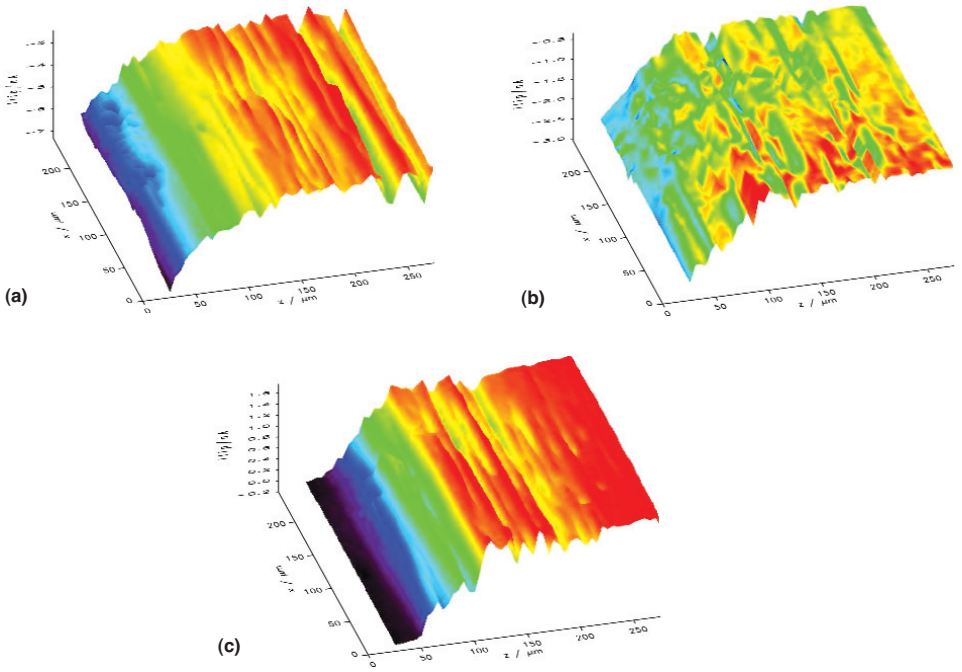

Figure 9—(a) Image of the proton concentration (E_{tip} = -0.3V, E_{sample} = 1.675 V vs. Ag/AgCl) close to the electrode (z_{elec} = 0 µm), the image was recorded by subsequent line scans in y direction (parallel to the electrode surface) at different heights above the electrode. (b) Image of the oxygen concentration (E_{tip} = -0.05V, E_{sample} = 1.675 V vs. Ag/AgCl). (c) Image at E_{sample} = 1.675V and E_{tip} = 1.1V vs. Ag/AgCl (hydrogen peroxide)

the proton concentration increases to more than double, which might be related to the slow diffusion of sulphuric acid.

From the image taken at 1.1 V one can conclude that H_2O_2 or a similar intermediate is involved in the oxygen evolution process on this sample. It is very unlikely that the measured current is related to hydrogen oxidation as it would otherwise be visible as an anodic current already at -0.05 V.

Because the image is taken in the anodic region, the concentration of H_2O_2 decreases towards the electrode and even vanishes to 0 near to the electrode (the current even changes to cathodic). From this it could be concluded that the H_2O_2 reaction at the electrode is fast and proceeding under current-limiting conditions. Just recently H_2O_2 has been detected in a similar experiment[24], generated from oxygen reduction on Pt/ Pd/Co in acidic media.

The images can be analysed and fitted to concentration profiles, which have been derived in theory for constant current processes (adapted after Bard and Faulkner[25]):

$$c(z,t) = c_b + \frac{i}{nFAD} \left\{ 2\left(\frac{Dt}{\pi}\right)^{1/2} \exp\left(-\frac{z^2}{4Dt}\right) - z\,erfc\left[\frac{z}{2(Dt)^{1/2}}\right] \right\} \quad [5]$$

Equation [5] is a solution of semi-infinite linear diffusion in absence of convection. The reason that the diffusion profile can nevertheless be described with it, is the occurrence of steady state (I and E are constant). The convection accelerates mass transport outside the Nernst diffusion layer preventing it to spreading out further, so that after a certain transition time t_t both potentiostatic and galvanostatic measurement methods result in the same concentration profiles.

From fitting the measured data, following parameters can be obtained: The diffusion coefficient D if the (local) current density is known (or vice versa j_{local} can be obtained), the surface concentration c_s, its normalization factor $X = c_s/c_b$ and the Nernst diffusion layer thickness δ, which describes mainly the influence of convection. δ can be calculated from a linear fit of concentration values near to the electrode intersecting with the bulk concentration value for a certain $z = \delta$. Another parameter is the bulk concentration c_b, The tip current value at far distance from the electrode (plateau in Figure 9) relates to it and determines a constant with which all the other current values can be mapped directly to concentrations (linear relationship).

The results from fitting are shown in Figure 10 and Table I.

For fitting Equation [5] to the proton concentration, a direct assignment of concentration to the measured current was possible due to the known proton concentration in the bulk solution, which was assumed to be 2 mol/ℓ (no SO_4^{2-} present). The diffusion coefficient was assumed to be that of sulphuric acid ($D=2.2\bullet10^{-5}$ cm²/s[26]). Two fitting parameters, the transition time tt_G and the local current density j_{loc} were fitted. All other values were calculated.

For oxygen the diffusion coefficient was also taken from literature ($D_{O2}= 1.9\bullet10^{-5}$ cm²/s[27]). For the unknown bulk concentration, direct fitting lead to divergence, thus it was estimated. By trial it was found that a value of 5 mmol/ℓ gave the most promising result. The transition time and local current density were fitted, and the rest of the values were calculated.

For hydrogen peroxide, the fitting was done to a virtual coordinate ($z'=z$-20 µm), otherwise negative concentrations would have resulted. Bulk concentration and diffusion constant were fitted, and the rest of the variables were calculated.

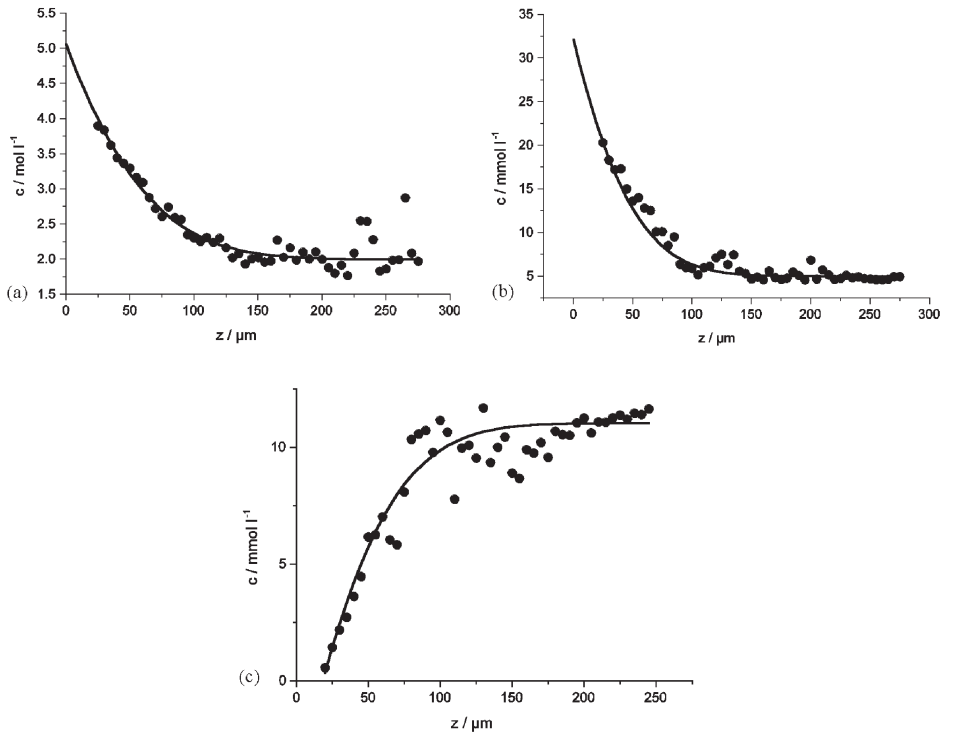

Figure 10—Fitting results, (a) proton concentration, (b) oxygen concentration, (c) hydrogen peroxide concentration

Table I

Fitting results for the 3 different detected species, including fixed parameters

Detected species	Fixed parameters	Resulting parameters and calculated variables				
		D / tt_G	δ	c_b	c_s / X	j_{loc}
H^+	D, c_b	- / 1.40 s	69 µm	-	5.1 mol ℓ-1 / 2.53	1.04 A/cm²
O_2	D	- / 0.91 s	55 µm	5 mmol l-1	32 mmol ℓ-1/ 6.42	0.02 A/cm²
H_2O_2	cs, j_{loc}	1.8•10-5 cm²s-1 1.03 s	55 µm	11 mmol l-1	-	-

The results in Table I show the following characteristics:

The build-up of the Nernst diffusion layer is a fast process for all species due to its very small extension (50–70 µm). The concentration of protons and especially that of oxygen increases substantially at the surface. Oxygen could be described as being present in the solution in supersaturation (above the solubility limit).

For the measured profile of protons, the fit shows that the local current density must be spatially dependent, otherwise the geometric current density (*ca.*7.5 mA/cm²) has to be the same. The same can also be argued for oxygen where, however, the difference is much smaller.

Hydrogen peroxide can be described to be present in considerable amounts.

Concentration images at constant height

Similarly to the previous methodology for YZ scans, the surface was approached in a different position, the tilt of the surface was eliminated with the precision gauges in both X and Y direction, and XY images were recorded 125 µm above the electrode plane.

First an overview was scanned (fast scan 500 x 500 µm, not shown here) to assure that the scan directions were parallel to the electrode. After that, a detailed section, where high electrochemical activity was expected, was chosen and rescanned at lower speed and higher precision.

For simplicity the images were generated such that dark colours indicate high concentrations while brighter colours indicate lower concentrations. The results can be seen in Figure 11.

From the images, it can seen that the concentrations measured vary substantially and seem to display similar features in the upper right corner, which can be seen as active region, were oxygen and protons are generated while hydrogen peroxide is consumed (analogous to Equation [3b]). The remaining parts of the images can be described as inactive regions where H_2O_2 could be generated (compare to H_2O_2 image in Figure 11).

Discussion

The AFM and the CAFM image indicate that the electrical properties of the composite electrode could lead to increased

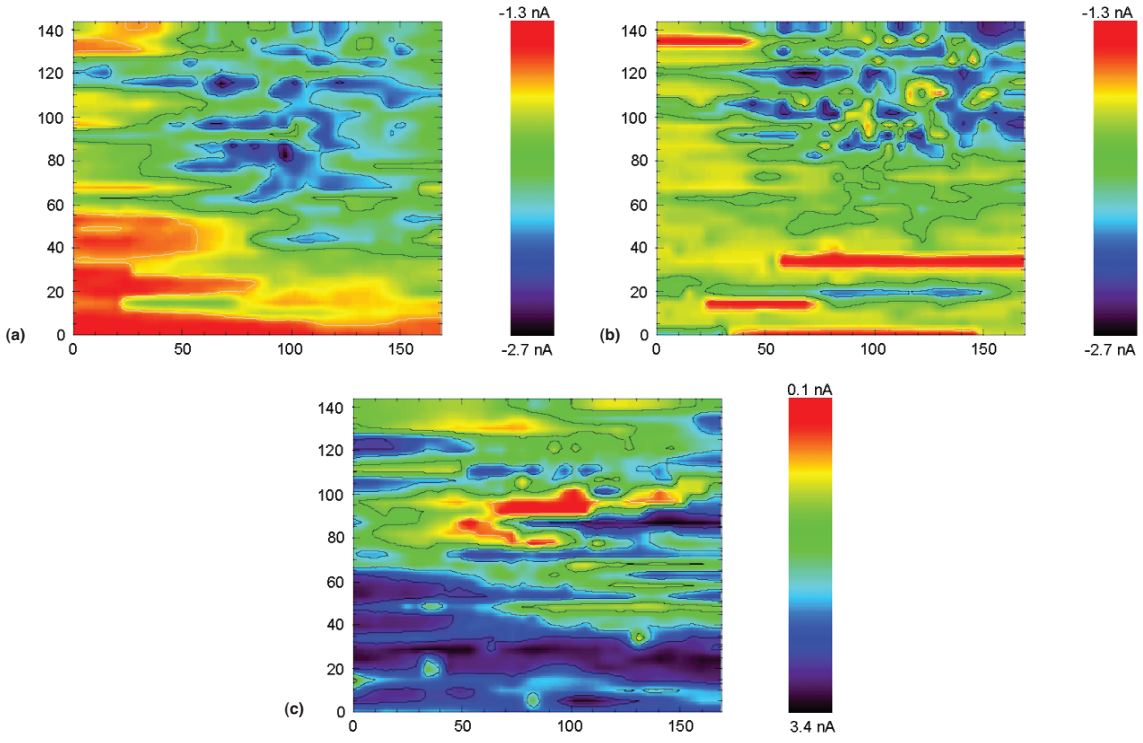

Figure 11—XY images 125 µm above the surface. Picture dimensions are in µm, (a) E_{sample} = 1.7V, E_{tip} = -0.3 V vs. Ag/AgCl (H^+), (b) E_{sample} = 1.7 V, E_{tip} = -0.05 V vs. Ag/AgCl (O_2), (c) E_{sample} = 1.7 V, E_{tip} = 1.1V vs. Ag/AgCl (H_2O_2)

current throughput at the boundaries between matrix and catalyst material. This supports the presented active boundary directly, especially because MnO_2 is not a good conductor, however, electrochemically active (compare with batteries).

From the measurements it can be concluded that mass transport has an influence on the measured system. This is due to the limiting current of H_2O_2 oxidation (Reaction [3b]), visible difference in proton concentration between bulk and surface and increasing oxygen concentration towards the surface.

This is also supported by the fitted concentration profiles, which show very high current densities for proton formation. This was concluded to be an indication of local processes with higher current densities than the average, or altogether heterogeneous current distribution. This could also be inferred from the horizontal XY images in Figure 11.

An expression of the concentration overpotential can be derived from two Tafel equations ($\eta = a' + b \log j$), one reflecting the current density at bulk concentration (no concentration overpotential), the other the current density at the actual surface concentration, from which the difference is the concentration overpotential (a' drops out):

$$\eta_C = b\left(\log j(c_b) - \log j(c_s)\right) = b\log\frac{j(c_b)}{j(c_s)} = b\log\frac{nFBk}{nFBk}\frac{c_b^a}{c_s^a} = ab\log\frac{c_b}{c_s} = -ab\log X \quad [6]$$

where b is the Tafel slope of the present mechanism, the other B describes all other expressions related to the mechanism, k is an electrochemical rate constant, nF the number of electrons transferred multiplied by the Faraday constant. $j(c_s)$ and $j(c_b)$ are the current density at surface and bulk concentration respectively. X is the ratio of c_s to c_b and a is the reaction order of the electrochemical reaction of the species of interest (O_2/H^+).

Protons that usually have larger reaction orders (a = -2/-1[13]) are thus expected to have a larger influence on concentration overpotential, while for oxygen one would expect a reaction order of a = -0.5/-0.25 with a lower concentration overpotential.

For a Tafel slope of 110 mV/dec (Figure 1), a reaction order of -2/-1 and X of 2.53 this results in a proton concentration overpotential of η_C = 89 mV/44 mV. For oxygen (X = 6.42) this results in η_C = 44 mV/22 mV.

High current densities combined with the very many small spots of the composite electrode should display edge effects in general, especially because the fraction of catalyst is very low (about 5 vol% of catalyst) and the overlap of diffusion field is small or negligible.

The direct boundary, however, is not accessible with SECM because of the topography (the catalyst particle protrudes above the surface). In the images it is therefore also impossible to decide whether it is the topography or the difference in reactivity that leads to the image contrasts. Many of the arguments presented here are not touched because they are based on comparisons of concentration of different species at equal positions in space.

The appearance of H_2O_2 as an intermediate (or similar species like $H_2S_2O_8$, O3, etc.) is interesting and surprising at the same time: if H_2O_2 was reacting under limiting current conditions (which is reasonable for the very high overpotential η = 1.7V-0.7 V = 1 V) where did it come from if it was not produced at the composite electrode?

If there were a MnO_2 catalyst sitting in the upper right corner it would be very logical that H_2O_2 was consumed at limiting current density, MnO_2 being a catalyst for H_2O_2 decomposition;. This reaction (Reaction [4]) can either happen as anodic reaction, or, if the catalyst particle is not well electrically connected as a redox reaction dissolving the MnO_2 and destroying the catalyst.

That, however, still does not answer where the H_2O_2 originally originates from. It could be that it is produced on the lead part of the electrode (Reaction [3c]) and is not visible in the proton image, because it can happen at much lower current density (about 95% of the surface is lead).

Then we would have a two-step two-material process just as it is presented earlier with the consequence that the boundaries would be especially active, because there the distance between both areas is closest and H_2O_2 could react directly further to oxygen. At distances far away from a catalyst particle the H_2O_2 would be transferred into the bulk solution, which would explain the considerable amount of H_2O_2 (of 10 mM).

Since Reaction [3c] would happen at limiting current, Reaction [4] would be potential determining which seem both reasonable for 1.675 V/1.7 V vs. Ag/AgCl (1.875 V/1.9 V vs. SHE). This is a very complex possible reaction scheme that could not happen at electrodes with homogenous properties.

The actual topography of the surface in that particular position, however, remains unknown, which would be essential information for the discussion (whether the inactive areas are in close proximity or further from the underlying surface).

If a levelling of the electrode surface could be achieved (which appears to be difficult because of the difference in hardness of both materials), the boundary would be directly accessible from relatively short distance, increasing the SECM image contrast.

This would clearly address the problem whether the hydrogen peroxide concentration would actually generally decrease towards the electrode (also on Pb) or not, relating to the question if the image contrasts in Figure 11 is due mainly to a topographical reason (MnO_2 sticks out, Pb is further away) or due to different reactions happening in different places. If that problem could be solved, the existence of a two-material two-step mechanism could be directly proven or disproved. As such it remains a suggestion that reflects and explains the measured data.

Related to the actual tankhouse environment such a combination would lead to hydrogen peroxide and oxygen gas forming in between the lead anode and the grown MnO_2 layer. Such circumstances would be a good explanation why that layer is only loosely attached and flakes off very easily in Zn electrowinning.

Although bubbles could not be seen or detected, it is nevertheless possible to assess the influence of convection with its key variable δ. The Nernst diffusion layer thickness is very small, but such small diffusion layers have been measured before for the oxygen evolution reaction[28]. SECM appears to be a good method to study convection at gas evolving electrodes, because it can detect the Nernst diffusion layer.

Conclusion

Scanning electrochemical microscopy (SECM) and conducting atomic force microscopy (CAFM) seem to be suitable tools to analyse electrochemical and electrical properties of composite electrodes.

With their help it was possible to show that some of the possible mechanisms presented do seem to happen at the electrode. It was concluded that both electrical properties and mass transport could have an influence on the performance of composite electrodes.

These special electronic properties and the high proton concentration build-up are good motivations for an additional internal iR drop or concentration overpotential respectively. These could probably be avoided by correct design (size and fraction of catalyst), if the assumption that the current passes mainly through the boundaries between matrix and catalyst is correct.

However, there was no direct proof for mechanisms resulting in special activity of the boundaries between matrix and catalyst, and for the mathematical model developed previously.

An intermediate has been detected and assigned to H_2O_2. A two-step two-material mechanism for that intermediate has been suggested on the basis of the SECM measurements. If H_2O_2 evolves as an intermediate here, it could be also a candidate for the oxygen evolution reaction on normal lead anodes.

Another interesting aspect of SECM is that it can measure and visualize the Nernst diffusion layer at gas-evolving electrodes. Despite the possibility that the noise of the generated bubbles would make such a measurement impossible, it is obviously possible to make images of that layer and fit the measured concentrations with the behaviour expected in theory.

For future work we intend to simulate both mass transfer and electrical properties to see whether it leads to similar supporting arguments.

References

1. Aromaa, J. and J.W. Evans. Electrowinning of metals. *Encyclopedia of Electrochemistry*, 2007. vol. 5, p. 159–265.
2. Beer, H.B. U.S. Pat. Appl. 549,194 (1966); U.S. Pat. 3,632,498 (1972); U.S. Pat. 3,711,385 (1973). 1966.
3. Beer, H.B. Eur. Pat. Appl. EP0046727; Eur. Pat. Appl. EP0087186, 1982.
4. Pajunen, L.A., Jari and Forsen, Olof., The effect of dissolved manganese on anode activity in electrowinning. *Hydrometallurgy 2003, Proceedings of the International Symposium honoring Professor Ian M. Ritchie*, Vancouver, BC, Canada, Aug. 24–27, 2003. vol. 2: p. 1255–1265.
5. Pletcher, D.W. and Frank, C. *Industrial Electrochemistry*. 2nd edn. 1990: Chapman and Hall.
6. Hrussanova, A.M., Dobrev, L., and Vasilev, S. Influence of temperature and current density on oxygen overpotential and corrosion rate of Pb-Co3O4, Pb-Ca-Sn, and Pb-Sb anodes for copper electrowinning: Part I. *Hydrometallurgy*, 2004. vol. 72: pp. 205–213.
7. Rashkov, S.D., Ts., Noncheva, Z., Stefanov, Y., Rashkova, B., and Petrova, M. Lead-cobalt anodes for electrowinning of zinc from sulfate electrolytes. *Hydrometallurgy*, 1999. vol. 52, pp. 223–230.
8. Dattilo, M.L., L. J. Merrlin composite anode technology for metal electrowinning. 2001.
9. Dattilo, M.L., L. J. Merrlin composite anodes for copper electrowinning. 1999.

10. Electrodes International, I., An insoluble titanium- lead anode for sulfate electrolytes, Electrodes International, Inc.
11. Gaertner, F., *et al*. The cold sprays process and its potential for industrial applications. *Journal of Thermal Spray Technology*, 2006. vol. 15, no. 2, pp. 223–232.
12. Cattarin, S. and Musiani, M. Electrosynthesis of nanocomposite materials for electrocatalysis. *Electrochimica Acta*, 2007. vol. 52, no. 8, pp. 2796–2805.
13. *Electrodes of conductive metallic oxides*, Part A and B, S. Trasatti (ed.). 1980/81, Elsevier scientific publishing company.
14. Schmachtel Sönke, T.M., Kontturi Kyösti, Forsén Olof, Barker, and Michael, H. Composite electrodes and MnOx for oxygen evolution in metal electrowinning. *European metallurgical conference 2007*. 2007. Düsseldorf.
15. Sloane, N.J.A. Kepler's conjecture confirmed. *Nature* (London), 1998. 395(6701): pp. 435–436.
16. Janssen, L.J.J. and Barendrecht, E. Mass transfer at a rotating ring-cone electrode and its use to determine supersaturation of gas evolved. *Electrochimica Acta*, 1984. vol. 29, no. 9: pp. 1207–12.
17. Stulik, K.A., Holub, C., Marecek, K., Vladimir and Kutner, Wlodzimierz., Microelectrodes. Definitions, characterization, and applications: (technical report). *Pure and Applied Chemistry*, 2000. vol. 72, pp. 1483–1492.
18. O'Hare, D., MacPherson, J.V., and Willows, A. On the microelectrode behaviour of graphite-epoxy composite electrodes. *Electrochemistry Communications*, 2002. vol. 4, no. 3, pp. 245–250.
19. Szunerits, S., Pust, S.E., and Wittstock, G. Multidimensional electrochemical imaging in materials science. *Analytical and Bioanalytical Chemistry*, 2007. vol. 389, no. 4, pp. 1103–1120.
20. Wilhelm, T. and Wittstock, G. Generation of periodic enzyme patterns by soft lithography and activity imaging by scanning electrochemical microscopy. *Langmuir*, 2002. vol. 18, no. 24, pp. 9485–9493.
21. Wittstock, G., Asmus, T., and Wilhelm, T. Investigation of ion-bombarded conducting polymer films by scanning electrochemical microscopy (SECM). *Fresenius J Anal Chem FIELD,* 2000. vol. 367, no. 4, pp. 346-51. FIELD Reference Number: FIELD Journal Code:9114077 FIELD Call Number:.
22. Atkins, P.W. *Physical Chemistry*, 6th Edition. 1998. 1014 pp.
23. Kaskiala, T. and Salminen, J. Oxygen solubility in industrial process development. *Industrial and Engineering Chemistry Research*, 2003. vol. 42, no. 8, pp. 1827–1831.
24. Shen, Y., Traeuble, M., and Wittstock, G. Detection of Hydrogen Peroxide Produced during Electrochemical Oxygen Reduction Using Scanning Electrochemical Microscopy. *Analytical Chemistry* (Washington, DC, United States), 2008. vol. 80, no. 3, pp. 750–759.
25. Larry, R. and Faulkner, A.J.B. *Electrochemical Methods Fundamentals and Application* Second Edition. 2001: John Wiley \& Sons, INC.
26. Lobo, V.M.M. *Handbook of electrolyte solutions Part A. physical science data*, V.M.M. Lobo (ed.). vol. 41. 1989, Amsterdam: Elsevier.
27. Juermann, G., Schiffrin, D.J., and Tammeveski, K. The pH-dependence of oxygen reduction on quinone-modified glassy carbon electrodes. *Electrochimica Acta*, 2007. vol. 53, no. 2, pp. 390–399.
28. Nefedov, V.G., Artyushenko, O.A., and Kashevarova, E.V. Mass transfer to horizontal gas-generating electrodes. *Russian Journal of Electrochemistry*, 2006. vol. 42, no. 6, pp. 638–642. ◆

